

## Vector resonances and electromagnetic nucleon structure

Robert A. Williams,\* Siegfried Krewald,<sup>†</sup> and Kevin Linen<sup>‡</sup>

*Continuous Electron Beam Accelerator Facility, Newport News, Virginia 23606*

(Received 7 September 1994)

Motivated by new, precise magnetic proton form factor data in the timelike region, a hybrid vector meson dominance (hVMD) formalism is employed to investigate the significance of excited vector meson resonances on electromagnetic nucleon structure. We find that the  $\rho(1700)$ ,  $\omega(1600)$ , and two previously unobserved states are required to reproduce the local structure seen in the new LEAR data just above the  $p\bar{p}$  threshold. We also investigate sensitivity to the  $\phi$  meson. The model dependence of our result is tested by introducing an alternative model which couples the isoscalar vector meson states to a hypothetical vector glueball resonance. We obtain nearly identical results from both models, except for  $G_E^n(q^2)$  in the spacelike region which is very sensitive to the glueball mass and the effective  $\phi NN$  coupling.

PACS number(s): 13.40.Gp, 12.40.Vv

### I. INTRODUCTION

Nucleon structure is a topic of fundamental importance in nuclear physics. The distribution of quarks and gluons bound by nonperturbative interactions inside the nucleon give rise to a complicated many-body structure which, except for very short distances where perturbative QCD (pQCD) applies, is up to the present time unsolvable from first principles. In order to make progress in understanding the nonperturbative features of nucleon structure, one has to resort to calculations based on phenomenological models.

Our analysis is motivated by new timelike proton magnetic form factor data which has been determined recently from measurements of the exclusive cross section for electron-positron production (annihilation) by proton-antiproton annihilation (production),  $p\bar{p} \leftrightarrow e^+e^-$ . The new precision data has been obtained for momentum transfers in the region  $8.9 \text{ GeV}^2 \leq q^2 \leq 13 \text{ GeV}^2$  (Fermilab E-760) [1] and in the vicinity of the proton-antiproton threshold (LEAR PS170) [2]. There is also new, but less precise timelike data (including one  $G_E^n$  point) from the FENICE experiment [3]. Perturbative QCD (pQCD) calculations are usually compared with data for spacelike momentum transfers larger than  $Q^2 \sim 10 \text{ GeV}^2$  [4,5]. The new Fermilab E-760 data confirm the predictions of perturbative QCD for the slope of magnetic form factor in the timelike region [1]. Several versions of the vector meson dominance (VMD) model [6–11], on the other hand, predict a slope of the mag-

netic form factor of the proton at the proton-antiproton threshold which is about five times smaller than the new low energy antiproton ring (LEAR) data. Given the apparent failure of the vector meson dominance model and the success of pQCD, the data have been used to derive a running coupling constant in the timelike region [1].

Ideally, one would like to calculate the nucleon form factors in terms of the underlying quark interactions. A quark model which incorporates the chiral symmetry of QCD, the Nambu Jona-Lasinio (NJL) model [12], has been developed quite successfully in recent years (reviews can be found in Refs. [13] and [14]). Generalizations of the model are able to generate nucleon and meson form factors [15,16] in good agreement with the experimental data for small spacelike momentum transfers. At large spacelike momentum transfers, however, a logarithmic divergence develops (see Fig. 7 of Ref. [17]), and the model must be regulated in some way. In the timelike region, applications of the NJL model are limited to relatively small excitation energies, because the model does not confine [14,18]. There are, of course, other microscopic models which have been successfully developed (such as constituent quark, skyrmion, bag models, etc.), each with its own set of virtues and shortcomings.

A less fundamental approach is to employ effective meson-nucleon interactions to study nucleon structure, especially in the timelike region where resonance phenomena is important. In this work, we investigate the effects of excited vector resonances on the electromagnetic nucleon form factors. Since the focus of this paper is on the timelike resonance structure of the nucleon, we neglect the evaluation of nonresonant meson loops which primarily effect the behavior of the spacelike form factors [19]. We employ a hybrid vector meson dominance (hVMD) formalism, which is a generalization of the model developed by Gari and Krümpelmann [20]. The model provides a smooth transition from the low- $q^2$  behavior predicted by VMD to the high- $q^2$  scaling behavior predicted by pQCD. The essential contribution of this work is to incorporate both timelike and spacelike

\*Present address: Department of Physics, Hampton University, Hampton, VA 23668.

<sup>†</sup>Present address: Forschungszentrum Jülich, Institut für Kernphysik, D-52428 Jülich, Germany.

<sup>‡</sup>Present address: Department of Physics, Benedict College, Columbia, SC 29204.

nucleon form factor data to determine the role of excited vector resonances which can be neglected in analyses based only on the spacelike data (such as in Ref. [20]). Although in this analysis we limit ourselves to a phenomenological model, we note that with the advent of new and forthcoming high quality data [1-3,21], there is a great opportunity and challenge for theorists to develop more realistic microscopic models.

In this work, we assume that the behavior of the data just above the  $p\bar{p}$  threshold is due to the effect of two nearby (previously unobserved) vector meson resonances (one below and one above threshold). We assign the isospin such that the lighter state is an isoscalar ( $\omega''$ ) and the heavier state is isovector ( $\rho''$ ). The masses, decay widths, and effective couplings of these states are treated as adjustable parameters. All other vector meson states, the  $\rho(770)$ ,  $\omega(784)$ ,  $\phi(1020)$ ,  $\omega'(1600)$ , and  $\rho'(1700)$  are given their physical masses and widths, each having two effective couplings (vector and tensor) which are fitted.

## II. HYBRID VECTOR MESON DOMINANCE

The basic assumption of hVMD is that the physical photon couples to the nucleon in either a hard perturbative mode (the direct term) or mediated by vector meson intermediate states (see Fig. 1). The electromagnetic nucleon form factors are defined by the usual current matrix element:

$$\langle p' | J_\mu^i | p \rangle \equiv \frac{g_i}{2} u(p') [F_1^i(q^2) \gamma_\mu + \frac{i\sigma_{\mu\nu}(p' - p)^\nu}{2M} \kappa_i F_2^i(q^2)] \mathcal{I}_i u(p) , \quad (1)$$

$$F_1^{IV}(q^2) = \left[ \sum_V^{\rho, \rho', \rho''} C_V \left( \frac{M_V^2}{M_V^2 - q^2 + iM_V \Gamma_V \Theta(q^2)} \right) F_1^V(q^2) \right] + C_\gamma^{IV} F_1^\gamma(q^2) , \quad (6)$$

$$F_1^{IS}(q^2) = \left[ \sum_V^{\omega, \omega', \omega'', \phi} C_V \left( \frac{M_V^2}{M_V^2 - q^2 + iM_V \Gamma_V \Theta(q^2)} \right) F_1^V(q^2) \right] + C_\gamma^{IS} F_1^\gamma(q^2) , \quad (7)$$

$$\kappa_{1V} F_2^{IV}(q^2) = \left[ \sum_V^{\rho, \rho', \rho''} \kappa_V C_V \left( \frac{M_V^2}{M_V^2 - q^2 + iM_V \Gamma_V \Theta(q^2)} \right) F_2^V(q^2) \right] + \kappa_\gamma^{IV} C_\gamma^{IV} F_2^\gamma(q^2) , \quad (8)$$

$$\kappa_{1S} F_2^{IS}(q^2) = \left[ \sum_V^{\omega, \omega', \omega'', \phi} \kappa_V C_V \left( \frac{M_V^2}{M_V^2 - q^2 + iM_V \Gamma_V \Theta(q^2)} \right) F_2^V(q^2) \right] + \kappa_\gamma^{IS} C_\gamma^{IS} F_2^\gamma(q^2) , \quad (9)$$

where  $C_V \equiv g_V/f_V$  is the effective coupling constant, with  $f_V$  the vector meson leptonic decay constant. The four effective couplings of the direct photon terms are determined by the charge and magnetic moment normalizations:

$$C_\gamma^{IV} \equiv \left( 1 - \sum_V^{\rho, \rho', \rho''} C_V \right) , \quad (10)$$

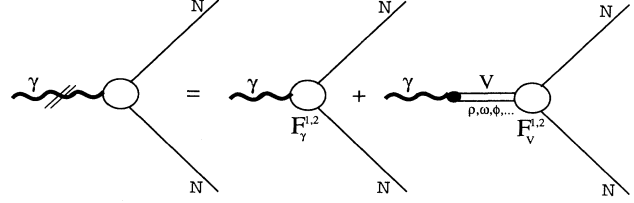


FIG. 1. Hybrid vector meson dominance picture of a physical photon coupling to the nucleon.

where the index  $i = IS, IV$  labels the isospin (0 or 1). The corresponding isospin operators are  $\mathcal{I}_{IS} = 1$  for isoscalar and  $\mathcal{I}_{IV} = \tau_3$  for isovector particles.  $q^2 = (p' - p)^2$  is the invariant momentum transfer of the photon, and  $g_i/2$  is the vector meson nucleon coupling constant. The Sachs electric and magnetic nucleon form factors are the standard linear combinations of the isospin form factors:

$$G_M^N(q^2) \equiv F_1^N(q^2) + F_2^N(q^2) , \quad (2)$$

$$G_E^N(q^2) \equiv F_1^N(q^2) + \frac{q^2}{4M^2} F_2^N(q^2) , \quad (3)$$

where  $N = p, n$  for the proton or neutron and

$$F_1^N(q^2) \equiv \frac{1}{2} [ F_1^{IS}(q^2) \pm F_1^{IV}(q^2) ] , \quad (4)$$

$$F_2^N(q^2) \equiv \frac{1}{2} [ \kappa_{1S} F_2^{IS}(q^2) \pm \kappa_{1V} F_2^{IV}(q^2) ] , \quad (5)$$

with the positive sign taken for the proton and negative sign for the neutron. Evaluating the diagrams of Fig. 1 we obtain the hVMD isospin form factors of the nucleon:

$$C_\gamma^{IS} \equiv \left( 1 - \sum_V^{\omega, \omega', \omega'', \phi} C_V \right) , \quad (11)$$

$$\kappa_\gamma^{IV} C_\gamma^{IV} \equiv \left( \kappa_{1V} - \sum_V^{\rho, \rho', \rho''} \kappa_V C_V \right) , \quad (12)$$

$$\kappa_\gamma^{IS} C_\gamma^{IS} \equiv \left( \kappa_{1S} - \sum_V^{\omega, \omega', \omega'', \phi} \kappa_V C_V \right) , \quad (13)$$

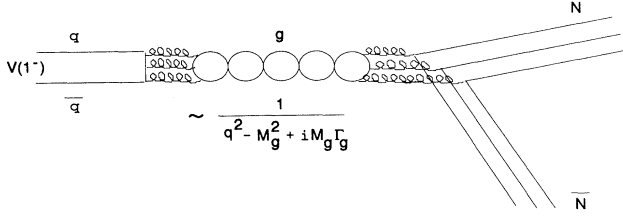


FIG. 2. Cartoon of a vector meson to glueball transition which subsequently couples to the nucleon. The meson to glueball transition is possible due to the intrinsic quark structure of the vector meson intermediate states. A glueball state will give the vector meson nucleon vertex function a resonance enhancement near the glueball mass.

so that

$$G_E^p(0) = 1, \quad G_M^p(0) = 1 + \frac{1}{2}(\kappa_{\text{IS}} + \kappa_{\text{IV}}), \quad (14)$$

$$G_E^n(0) = 0, \quad G_M^n(0) = \frac{1}{2}(\kappa_{\text{IS}} - \kappa_{\text{IV}}). \quad (15)$$

The direct coupling form factors ( $F_{1,2}^\gamma$ ) are chosen such that the low- $q^2$  behavior is given by a  $\rho$ -dominance monopole with a transition to the correct pQCD scaling behavior at high  $q^2$  [20]. The vector meson to quark transition scale is set by the parameter  $\lambda$ :

$$F_n^\gamma(q^2) = \left[ \frac{M_\rho^2(M_\rho^2 + \Gamma_\rho^2)}{(q^2 - M_\rho^2)^2 + (M_\rho\Gamma_\rho)^2} \right]^{1/2} \left( \frac{\lambda^2}{\lambda^2 + |q^2|} \right)^n \quad (n = 1, 2). \quad (16)$$

The specification of the vector meson nucleon vertex function is a model dependent assumption. Following Gari and Krümpelmann, in our first model ( $\mathcal{M}1$ ) we take

$$\underline{\mathcal{M}1}: \quad F_n^V(q^2) = F_n^\gamma(q^2) \quad (n = 1, 2) \quad (\forall_V). \quad (17)$$

Because the vector mesons have intrinsic quark (color) structure, an interesting possibility exists for transitions

to gluonic resonances (glueballs), (see Fig. 2). To investigate the potential influence of a vector glueball on EM nucleon structure, we allow for such a resonance and test its effect on the form factors and the stability of the hVMD parametrization (i.e., test the model dependent sensitivity of the effective couplings). If a glueball exists, it should be an isosinglet, hence our second model ( $\mathcal{M}2$ ) enhances the effective isoscalar couplings by producing a gluonic resonance in the meson-nucleon vertex function:

$$\underline{\mathcal{M}2}: \quad F_n^{\text{IS}}(q^2) = \left( \frac{M_g^2}{M_g^2 - q^2 + i M_g \Gamma_g \Theta(q^2)} \right) F_n^g(q^2) \quad (n = 1, 2) \quad (\forall_{\text{IS}}), \quad (18)$$

$$F_n^{\text{IV}}(q^2) = F_n^\gamma(q^2) \quad (n = 1, 2) \quad (\forall_{\text{IV}}), \quad (19)$$

where the glueball-nucleon vertex function is parametrized by a monopole:

$$F_n^g(q^2) = \frac{\Lambda_g^2}{(\Lambda_g^2 + |q^2|)} \quad (n = 1, 2). \quad (20)$$

All of the isospin form factors and vertex functions are normalized to unity at  $q^2 = 0$  so that the charge and magnetic moment normalizations of the nucleon are preserved. We note that the glueball couplings in the  $\mathcal{M}2$  parametrization have been absorbed into the effective isoscalar coupling constants. We allow for a nonzero  $\phi$ -nucleon coupling in both models since the OZI rule may be violated if, for example, the nucleon has a nonzero ( $s\bar{s}$ ) distribution.

We summarize the parametrizations of models  $\mathcal{M}1$  and  $\mathcal{M}2$  in Table I. A single valued entry in any column is common between  $\mathcal{M}1$  and  $\mathcal{M}2$ . The effective couplings appear to be relatively insensitive to the hypothetical glueball, except for the couplings of the  $\phi$  meson. We note that the  $\mathcal{M}1$  parametrization approximately satisfies:

$$C_\gamma^{\text{IV}} = 1, \quad C_\gamma^{\text{IS}} = 0, \quad (21)$$

TABLE I. Parameters of the hybrid vector meson dominance models  $\mathcal{M}1$  and  $\mathcal{M}2$ . The direct  $F_{1,2}^\gamma$  form factors have scale parameter  $\lambda = 2.0$  GeV and the glueball functions  $F_{1,2}^g$  have  $\Lambda_g = 1.0$  GeV. Also,  $\kappa_{\text{IS}} = -0.12$  and  $\kappa_{\text{IV}} = 3.706$  are fixed by the proton and neutron magnetic moments:  $\mu_p = 1 + \frac{1}{2}(\kappa_{\text{IS}} + \kappa_{\text{IV}})$ ,  $\mu_n = \frac{1}{2}(\kappa_{\text{IS}} - \kappa_{\text{IV}})$ . Masses and widths of speculated states were fit (underlined values). The starred values were fixed by low energy  $\pi N$  scattering analyses [27,28], and the numbers in parentheses are the physical, experimental masses, and decay widths of well-established resonances.

$V$	$C_V$		$\kappa_V$		$M_V$ (GeV)		$\Gamma_V$ (GeV)		
	$\mathcal{M}1$	$\mathcal{M}2$	$\mathcal{M}1$	$\mathcal{M}2$	$\mathcal{M}1$	$\mathcal{M}2$	$\mathcal{M}1$	$\mathcal{M}2$	
$\rho$	0.4					(0.776)		(0.153)	
$\rho'$	-2.0					(1.70)		(0.235)	
$\rho''$	1.6					2.15		0.22	
$\omega$	0.2					(0.784)		(0.010)	
$\omega'$	1.2					(1.60)		(0.100)	
$\omega''$	-0.3					<u>1.85</u>	<u>1.83</u>	<u>0.01</u>	
$\phi$	-0.1	0.3	-2.0	3.0		(1.02)		(0.004)	
$g$	-	1	-	1	-		1.5	-	0.2

which by Eqs. (10)–(13) implies the following sum-rules on the vector meson couplings:

$$\sum_V^{\rho, \rho', \rho''} C_V = 0, \quad (22)$$

$$\sum_V^{\omega, \omega', \omega'', \phi} C_V = 1, \quad (23)$$

$$\sum_V^{\omega, \omega', \omega'', \phi} \kappa_V C_V = \kappa_{\text{IS}}. \quad (24)$$

The physical interpretation is that the net isovector charge on the nucleon is due to its quark structure (implied by the direct photon coupling), whereas the nucleon's net isoscalar charge arises due to its coupling to the isoscalar vector mesons. Although these sum-rules are empirical, they could be assumed as a constraint in the fitting procedure to eliminate three degrees of freedom in each parametrization.

In Table II, we compute the contribution of each meson state to the the net charge radius of the proton and neutron from the relation:

$$\langle r_N^2 \rangle \equiv 6 \left. \frac{\partial G_E^N(q^2)}{\partial q^2} \right|_{q^2=0} \quad (N = p, n), \quad (25)$$

$$= \left[ \sum_V^{\text{IS}} \pm \sum_V^{\text{IV}} \right] r_N^2(V), \quad (26)$$

where the positive/negative sign corresponds to the proton/neutron. Taking the derivative of  $G_E^N(q^2)$ , we find the expression (for model  $\mathcal{M}1$ ):

$$r_N^2(V) = 3 C_V \left[ \frac{1}{M_V^2} + \frac{\kappa_V}{4M_N^2} + \left( \frac{1}{M_\rho^2} + \frac{1}{\lambda^2} \right) \right], \quad (27)$$

which we use to evaluate the elements of Table II. Note the strong cancellation between the  $\rho'$  and  $\rho''$  isovector states. Also, it is interesting that since we find  $C_\omega \ll C_{\omega'}$ , the  $\omega'(1600)$  resonance contributes more strongly to the net isoscalar radius than the substantially lighter ground state  $\omega$ .

TABLE II. Charge radius contributions from each vector meson resonance for model  $\mathcal{M}1$ . The net charge radii of the proton and neutron, given by Eq. (26), are  $\langle r_p^2 \rangle = 0.67 \text{ fm}^2$  and  $\langle r_n^2 \rangle = -0.096 \text{ fm}^2$ .

$V$	$r_N^2(V) \text{ (fm}^2\text{)}$
$\rho$	0.248
$\rho'$	-0.534
$\rho''$	0.408
$\gamma_{\text{IV}}$	0.261
$\sum_V^{\text{IV}} r_N^2(V)$	0.383
$\omega$	0.084
$\omega'$	0.311
$\omega''$	-0.076
$\phi$	-0.031
$\gamma_{\text{IS}}$	-0.001
$\sum_V^{\text{IS}} r_N^2(V)$	0.287

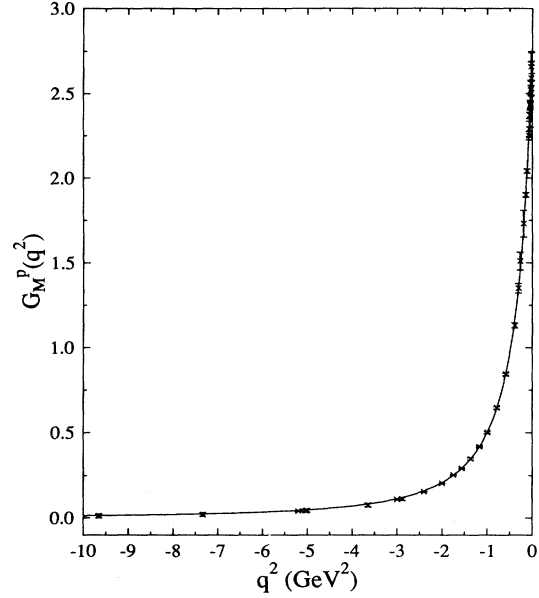


FIG. 3. Model  $\mathcal{M}1$  proton magnetic form factor,  $G_M^p$  in the spacelike region. The data are from Ref. [25].

In Figs. 3 and 4 we display our  $\mathcal{M}1$  model result for  $G_M^p(q^2)$  in the spacelike and timelike regions, respectively. We plot  $\mathcal{M}1$  in the spacelike region for  $G_E^p(q^2)$  and  $G_M^n(q^2)$  in Figs. 5 and 6, respectively. The parametrization gives a very good account of the available data. Our primary result is that we find the excited vector meson states  $\rho'(1700)$ ,  $\omega'(1600)$ ,  $\rho''(2150)$ , and  $\omega''(1850)$  are necessary to give a detailed account of the  $G_M^p$  data just above the  $p\bar{p}$  threshold. The  $\rho''(2150)$  and  $\omega''(1850)$  are previously unobserved states which are not neces-

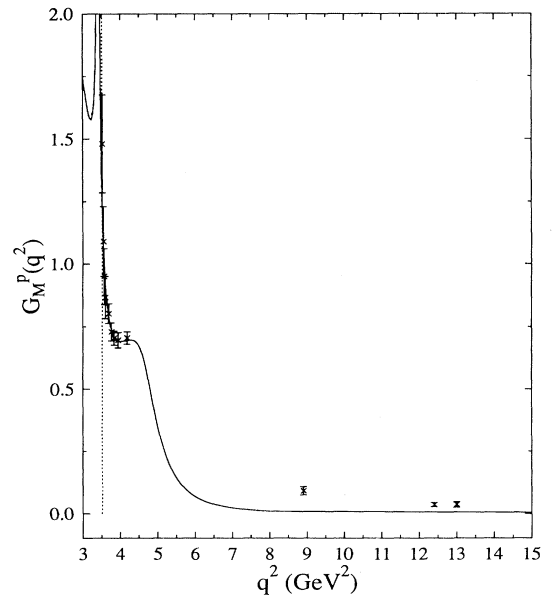


FIG. 4. Model  $\mathcal{M}1$  proton magnetic form factor,  $G_M^p$  in the timelike region. The data are from Refs. [1–3].

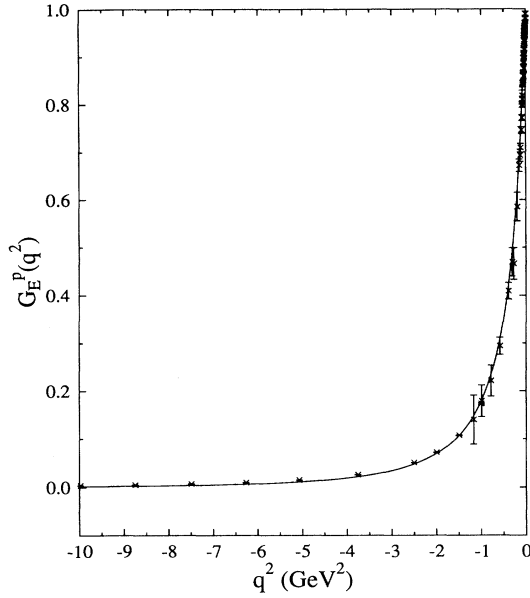


FIG. 5. Model  $M1$  proton electric form factor,  $G_E^p$  in the spacelike region. The data are from Ref. [25].

sarily vector mesons (e.g., a  $p\bar{p}$  molecular resonance or bound state, glueballs, etc.). Within a phenomenological framework, it is impossible to address the structure of these additional states, however, this analysis does at least provide support for their existence. In Figs. 7–9 the  $M2$  model prediction is shown to be nearly identical with the  $M1$  result in the physical region of the  $p\bar{p} \leftrightarrow e^+e^-$  reaction, but substantially different below the  $p\bar{p}$  threshold. Note the enhancement of the isoscalar vec-

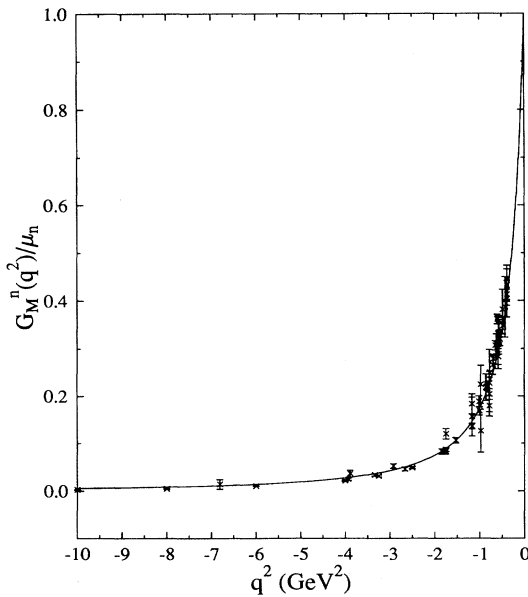


FIG. 6. Model  $M1$  neutron magnetic form factor,  $G_M^n$  in the spacelike region. The data are from Ref. [26].

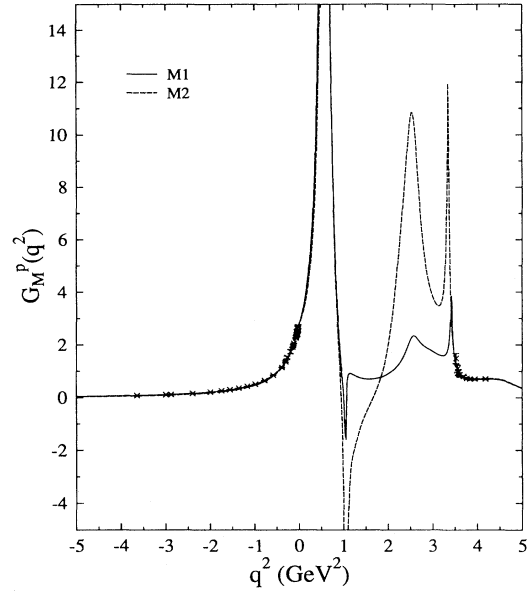


FIG. 7. Global view of models  $M1$  and  $M2$  for the proton magnetic form factor,  $G_M^p$ . The data are from Refs. [1–3,25].

tor meson peaks in model  $M2$ . Our final result, displayed in Figs. 10 and 11, shows a comparison of both model predictions for  $G_E^n(q^2)$  in the spacelike and timelike regions respectively. In the spacelike region of  $G_E^n$ , we also plot a parametrization of the most recent data deduced by Platchkov *et al.* [22] from an analysis of the elastic deuteron  $d(e, e')$  reaction (with an extraction based on a Paris potential deuteron wave function). Platchkov used the empirical form:

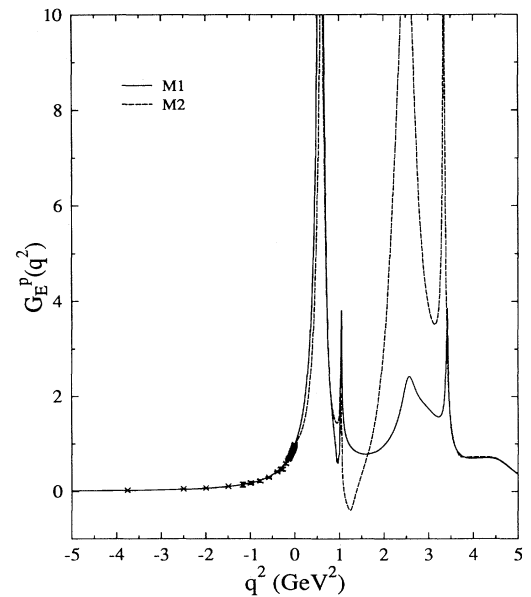


FIG. 8. Global view of models  $M1$  and  $M2$  for the proton electric form factor,  $G_E^p$ . The data are from Ref. [25].

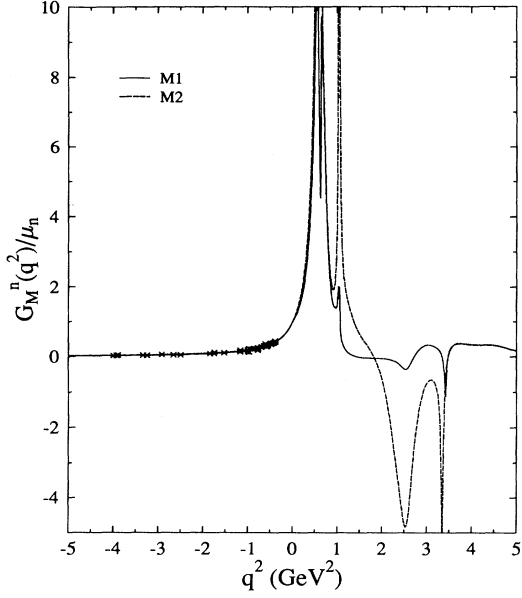


FIG. 9. Global view of models  $M1$  and  $M2$  for the neutron magnetic form factor,  $G_M^n$ . The data are from Ref. [26].

$$G_E^n(q^2) = -a \mu_n \tau G_D(q^2) (1 + b\tau)^{-1}, \quad (28)$$

with  $a = 1.25$ ,  $b = 18.3$ ,  $\mu_n = -1.913$ ,  $\tau = \frac{-q^2}{4M^2}$ , and  $G_D(q^2)$  is the standard dipole parametrization of  $G_E^p(q^2)$ . We note that there is a large variation in the Platchkov parametrization of  $G_E^n$  depending on the model deuteron wave function [22–24]. In both models,  $G_E^n$  is sensitive

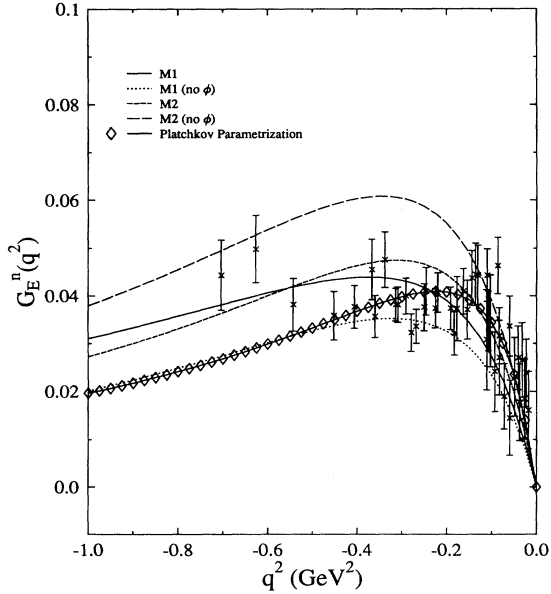


FIG. 10. The spacelike neutron electric form factor,  $G_E^n$  for both models  $M1$  and  $M2$ . Note the sensitivity to the  $\phi$ -meson coupling. The data are from Refs. [22–24].

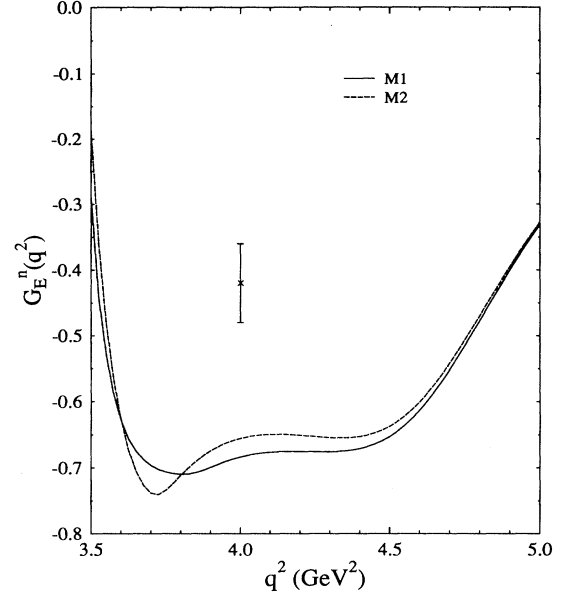


FIG. 11. The timelike neutron electric form factor,  $G_E^n$  for both models  $M1$  and  $M2$ . The data point is from Ref. [3].

to the effective  $\phi$ -nucleon couplings. We note that the  $\phi$  meson does not significantly enhance the quality of our fits to the other form factors and only has a potentially observable effect on spacelike  $G_E^n$ . An interesting result is that the  $M2$  model result for  $G_E^n$  in the spacelike region shows a large sensitivity to the glueball mass, which we have arbitrarily taken to be  $M_g = 1.5$  GeV. We observe (but do not show) that the glueball state tends to enhance/suppress  $G_E^n$  for large/small  $M_g$ . The sensitivity we observe due to the  $\phi$  meson and glueball is largely academic since it is probably not possible to extract information unambiguously about these novel contributions to the isoscalar current with only one observable ( $G_E^n$ ), especially since the spacelike behavior is affected by other mechanisms (such as meson loops, which have been neglected here). The most general conclusion to be drawn is that  $G_E^n$  is very sensitive to isoscalar admixtures and caution should be taken when trying to assess relative contributions from different mechanisms. In any event, we anxiously await new precision data for spacelike  $G_E^n$  from CEBAF [21] which will challenge and help theorists to build more realistic, quantitative models of nucleon structure.

In conclusion, we have investigated the effect of vector resonances on the electromagnetic nucleon form factors in both spacelike and timelike momentum transfer regions. The local behavior of the new LEAR data just about the  $p\bar{p}$  threshold suggests the existence of two new vector meson resonances with masses around 1.85 GeV and 2.15 GeV (which we denote  $\omega''$  and  $\rho''$ , respectively). Also, we find large effective couplings for the  $\omega'(1600)$  and  $\rho'(1700)$  resonances. The model parameters seem to be stable with respect to specific model assumptions (such as the existence of a glueball, its mass, and the form of the vector meson nucleon form factor). Because

of large cancellations between the various excited vector mesons, the net effect is only a modest contribution to the spacelike behavior, and hence models neglecting these excited states (such as in Ref. [20]) can produce similar spacelike results. Although largely an academic exercise, the novel (speculative)  $\phi$ -meson and glueball mechanisms studied in this work enhance our appreciation for the general complexity of nucleon structure and hence the importance of precision measurements which are scheduled to be performed at CEBAF in the near future [21].

#### ACKNOWLEDGMENTS

The authors thank Nathan Isgur, Franz Gross, and Warren Buck for their interest in this work. One of the authors (S.K.) thanks Nathan Isgur and Franz Gross for their hospitality and financial support during his visit at CEBAF. R.A.W. acknowledges support from NSF Grant No. HRD-9154080 and appreciates discussions on  $G_E^n$  and  $T_A^b$  with Tom Eden.

- 
- [1] T.A. Armstrong *et al.*, Phys. Rev. Lett. **70**, 1212 (1991).  
 [2] G. Bardin *et al.*, Phys. Lett. B **255**, 149 (1991); **257**, 514 (1991).  
 [3] E. Lippi, Nucl. Phys. **A558**, 165c (1993).  
 [4] G.P. Lepage and S.J. Brodsky, Phys. Rev. Lett. **43**, 545 (1979); Phys. Rev. D **22**, 2157 (1980).  
 [5] N.G. Stefanis and M. Bergmann, Phys. Rev. D **47**, R3685 (1993).  
 [6] M. Gell-Mann and F. Zachriassen, Phys. Rev. **124**, 953 (1961).  
 [7] J.J. Sakurai, *Currents and Mesons* (University of Chicago Press, Chicago, 1969).  
 [8] T.H. Bauer *et al.*, Rev. Mod. Phys. **50**, 161 (1978).  
 [9] T. Massam and A. Zichichi, Nuovo Cimento **43**, 1137 (1967).  
 [10] J.G. Koerner and M. Kuroda, Phys. Rev. D **16**, 2165 (1977).  
 [11] S. Dubnicka and E. Etim, Nuovo Cimento A **100**, 1 (1988).  
 [12] Y. Nambu and G. Jona-Lasinio, Phys. Rev. **122**, 345 (1961).  
 [13] S.P. Klevansky, Rev. Mod. Phys. **64**, 649 (1992).  
 [14] U. Vogl and W. Weise, Prog. Part. Nucl. Phys. **27**, 195 (1991).  
 [15] P. Alberto *et al.*, Phys. Lett. B **208**, 75 (1988).  
 [16] V. Bernard and U.G. Meissner, Phys. Rev. Lett. **61**, 2296 (1988).  
 [17] V. Dmitransinovic, R.H. Lemmer, and R. Tegen, Comm. Nucl. Part. Phys. **21**, 71 (1993).  
 [18] S. Krewald, K. Nakayama, and J. Speth, Phys. Lett. B **272**, 190 (1991).  
 [19] The neglect of meson loops essentially renormalizes the effective vector meson couplings of the model since the resulting charge and magnetic moment sum rules (i.e., normalization conditions) are saturated only by VM resonances and a direct photon coupling.  
 [20] M. Gari and W. Krümpelmann, Z. Phys. A **322**, 689 (1985); Phys. Lett. B **173**, 10 (1986); *ibid.* **274**, 159 (1992).  
 [21] CEBAF Experiment E93-038, Richard Madey, Hampton University.  
 [22] S. Platchkov *et al.*, Nucl. Phys. **A508**, 343c (1990); **A510**, 740 (1990).  
 [23] T. Eden, "The Electric Form Factor of the Neutron at  $Q^2 = 0.255 \text{ GeV}^2$  from the  $d(\bar{e}, e'\bar{n})p$  Reaction," dissertation, Kent State, 1993.  
 [24] T. Eden *et al.*, Phys. Rev. C **50**, R1749 (1994).  
 [25] Spacelike  $G_M^p$  and  $G_E^p$  data taken from G. Höhler *et al.*, Nucl. Phys. **B114**, 505 (1976); R. G. Arnold *et al.*, Phys. Rev. Lett. **57**, 174 (1986).  
 [26] Spacelike  $G_M^n$  data taken from A. Lung *et al.*, Phys. Rev. Lett. **70**, 718 (1993); A. S. Esausov *et al.*, Sov. J. Nucl. Phys. **45**, 258 (1987); S. Rock *et al.*, Phys. Rev. Lett. **49**, 1139 (1982); W. Bartel *et al.*, Nucl. Phys. **B58**, 429 (1973); K. M. Hanson *et al.*, Phys. Rev. D **8**, 753 (1973); W. Albrecht *et al.*, Phys. Lett. **26B**, 642 (1968); J. R. Dunning *et al.*, Phys. Rev. **141**, 1286 (1966); P. Stein *et al.*, Phys. Rev. Lett. **16**, 592 (1966); E. B. Hughes *et al.*, Phys. Rev. **139**, B458 (1965); C. W. Akerlof *et al.*, Phys. Rev. **135**, B810 (1964).  
 [27] G. Höhler and E. Pietarinen, Nucl. Phys. **B95**, 210 (1975); **B216**, 334 (1983).  
 [28] W. Grein and P. Kroll, Nucl. Phys. **A338**, 332 (1980).